

# **NON-LINEAR QUANTUM COHERENCE EFFECTS IN DRIVEN MESOSCOPIC SYSTEMS**

V. E. Kravtsov

*The Abdus Salam International Centre for Theoretical Physics, Strada Costiera 11, 34100 Trieste,  
Italy.*

*Landau Institute for Theoretical Physics, 2 Kosygina Street, 117940 Moscow, Russia*



## Contents

1. Introduction	5
2. Weak Anderson localization in disordered systems	5
2.1. Drude approximation	6
2.2. Beyond Drude approximation.	7
2.3. Weak localization correction.	9
3. Non-linear response to a time-dependent perturbation	12
3.1. General structure of nonlinear response function.	13
3.2. Approximation of single photon absorption/emission	15
4. Quantum rectification by a mesoscopic ring.	16
5. Diffusion in the energy space.	23
6. Quantum correction to absorption rate.	26
7. Weak dynamic localization and no-dephasing points.	30
8. Conclusion and open questions	34
References	35



## 1. Introduction

Over the last two decades theory and experiment on quantum disordered and chaotic systems have been an extremely successful field of research. The milestones on this route were:

- Weak Anderson localization in disordered metals
- Universal conductance fluctuations
- Application of random matrix theory to quantum disordered and chaotic systems

However the mainstream of research was so far limited to a *linear* response of quantum systems where the kinetic and thermodynamic properties are calculated essentially at equilibrium. The main goal of this course of lectures is to develop a theory of *nonlinear* response to a time-dependent perturbation in the same way as the theory of Anderson localization and mesoscopic phenomena. It will require an extension of an existing methods to *non-equilibrium phenomena*.

The four lectures will include the following topics:

- Perturbative theory of weak Anderson localization
- Keldysh formulation of nonlinear response theory
- Mesoscopic rings under AC pumping and quantum rectification
- Theory of weak dynamic localization in quantum dots

## 2. Weak Anderson localization in disordered systems

In this section we consider the main steps in the calculus of weak localization theory [1, 2]. The main object to study is the frequency-dependent conductivity

$$\begin{aligned} \sigma_{\alpha\beta}(\omega) &= \int_{-\infty}^{+\infty} \frac{d\varepsilon}{4\pi\omega} [f(\varepsilon) - f(\varepsilon - \omega)] \\ &\times \int \frac{d\mathbf{r}d\mathbf{r}'}{Vol} \langle e\hat{v}_\alpha (G^R - G^A)_{\mathbf{r},\mathbf{r}';\varepsilon} e\hat{v}_\beta (G^R - G^A)_{\mathbf{r}',\mathbf{r};\varepsilon-\omega} \rangle \end{aligned} \quad (2.1)$$

where  $G_{\mathbf{r}',\mathbf{r};\varepsilon}^{R/A}$  are retarded (advanced) electron Green's functions,  $f(\varepsilon)$  is the Fermi energy distribution function and  $\hat{v}_\alpha$  is the velocity operator. One can

convince oneself using the representation in terms of exact eigenfunctions  $\Psi_n(\mathbf{r})$  and exact eigenvalues  $E_n$

$$G_{\mathbf{r}',\mathbf{r};\varepsilon}^{R/A} = \sum_n \frac{\Psi_n(\mathbf{r})\Psi_n^*(\mathbf{r}')}{\varepsilon - E_n \pm i0} \quad (2.2)$$

that Eq.(2.1) reduces to a familiar Fermi Golden rule expression:

$$\sigma_{\alpha\beta}(\omega) = 2\pi \sum_{E_n > E_m} \langle n|J_\alpha|m\rangle \langle m|J_\beta|n\rangle \delta(E_n - E_m - \omega) \frac{f_{E_m} - f_{E_n}}{E_n - E_m} \quad (2.3)$$

Eq.(2.2) is convenient to prove exact identities but is useless for practical calculus. In disordered systems with the momentum relaxation time  $\tau$  the following expression for the disorder average Green's function is very useful:

$$\langle G^{R/A} \rangle_\varepsilon = \frac{1}{\varepsilon - \xi_{\mathbf{p}} \pm \frac{i}{2\tau}}. \quad (2.4)$$

where  $\xi_{\mathbf{p}} = \varepsilon(\mathbf{p}) - E_F$  is related with the electron dispersion law  $\varepsilon(\mathbf{p})$  relative the Fermi energy  $E_F$ . In what follows we will assume  $\xi = \xi_p$  depending only on  $|\mathbf{p}|$ . Then  $\xi$  and the unit vector of the direction of electron momentum  $\mathbf{n}$  constitute a convenient variables of integration over  $\mathbf{p}$ :

$$\int ... d\mathbf{p} \rightarrow \int \nu(\xi) d\xi \int d\mathbf{n}... \quad (2.5)$$

For a typical metal with  $E_F$  far from the band edges and the energy scale of interest  $\varepsilon \ll E_F$  the density of states  $\nu(\xi)$  can be approximated by a constant  $\nu = \nu(0)$  at the Fermi level and the integration over  $\xi$  can be extended over the entire real axis  $(-\infty, +\infty)$ .

### 2.1. Drude approximation

The simplest diagrams for the frequency-dependent conductivity are shown in Fig.1. The diagrams Fig.1a,b are given by the integrals

$$\int d\mathbf{n} v_\alpha v_\beta \int_{-\infty}^{+\infty} \frac{d\xi}{(\varepsilon - \xi \pm \frac{i}{2\tau})(\varepsilon - \omega - \xi \pm \frac{i}{2\tau})} = 0 \quad (2.6)$$

where  $v_\alpha \approx v_F n_\alpha$ .

It is important that the integral over  $\xi$  is the pole integral with all poles in the same complex half-plane. This is why such integrals are equal to zero. In contrast to that the diagrams of Fig.1c,d that contain both retarded ( $G^R$ ) and advanced ( $G^A$ ) Green's functions correspond to a similar integral with poles lying

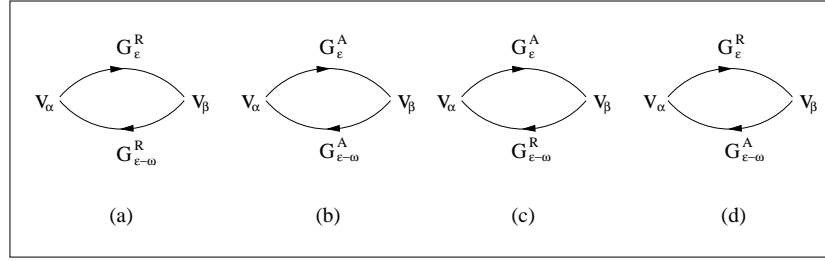


Fig. 1. Diagrams for the Drude conductivity.

in *different* half-planes of  $\xi$ . Such an integral over  $\xi$  can be done immediately using the residue theorem:

$$\int_{-\infty}^{+\infty} \frac{d\xi}{(\varepsilon - \xi \pm \frac{i}{2\tau})(\varepsilon - \omega - \xi \mp \frac{i}{2\tau})} = \frac{2\pi\tau}{(1 - i\omega\tau)}. \quad (2.7)$$

The angular integral is trivial:

$$\int d\mathbf{n} v_\alpha v_\beta = v_F^2 \frac{\delta_{\alpha\beta}}{d}, \quad (2.8)$$

where  $d$  is the dimensionality of space.

Now all what we need to compute  $\sigma_{\alpha\beta}$  using the simplest diagrams of Fig.1 is the identity:

$$\int_{-\infty}^{+\infty} [f(\varepsilon) - f(\varepsilon - \omega)] d\varepsilon = -\omega. \quad (2.9)$$

This identity holds for all functions  $f(\varepsilon)$  obeying the Fermi boundary conditions  $f(\varepsilon) \rightarrow 0$  at  $\varepsilon \rightarrow +\infty$  and  $f(\varepsilon) \rightarrow 1$  at  $\varepsilon \rightarrow -\infty$ .

The result of the calculations is the Drude conductivity:

$$\sigma_{\alpha\beta}^{(D)} = \frac{e^2 \nu D_0}{1 + (\omega\tau)^2} \delta_{\alpha\beta}, \quad (2.10)$$

where  $D_0 = v_F^2 \tau / d$  is the diffusion coefficient.

## 2.2. Beyond Drude approximation.

The diagrams that were not included in the Drude approximation of Fig.1 contain *cross-correlations* between the exact electron Green's functions  $G^R$  and  $G^A$  which arise because both of them see the *same* random impurity potential  $U(\mathbf{r})$ .

We make the simplest approximation of this potential as being the random Gaussian field with zero mean value and zero-range correlation function:

$$\langle U(\mathbf{r})U(\mathbf{r}') \rangle = \frac{\delta(\mathbf{r} - \mathbf{r}')}{2\pi\nu\tau}. \quad (2.11)$$

The simplest diagrams beyond the Drude approximation are the ladder series shown in Fig.2. The dotted line in these diagrams represent the momentum

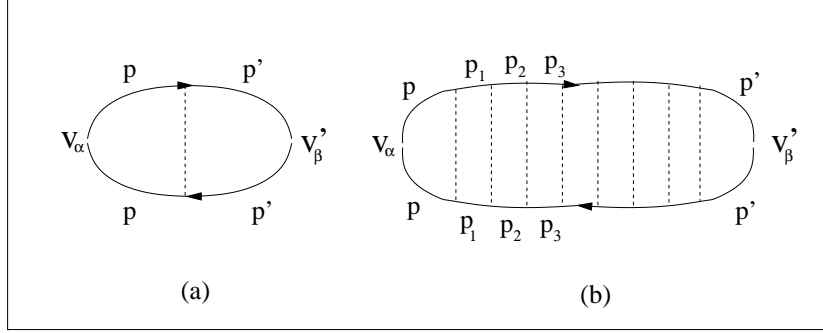


Fig. 2. Ladder diagrams.

Fourier transform of correlation function  $\langle U(\mathbf{r})U(\mathbf{r}') \rangle$  which is a constant  $1/2\pi\nu\tau$  independent of the momentum transfer  $\mathbf{p} - \mathbf{p}'$ . This makes the quantities  $v_\alpha$  and  $v'_\beta$  completely independent of each other. Then the angular integration

$$\int d\mathbf{n} v_\alpha = 0 \quad (2.12)$$

results in vanishing of all the ladder diagrams of Fig.2.

The next diagram with cross correlations contain an intersection of dotted lines (see Fig.3).

In contrast to a diagram with two parallel dotted lines where all integrations over momenta are independent, here the momentum conservation imposes a constraint:

$$\mathbf{p} + \mathbf{p}' = \mathbf{p}_1 + \mathbf{p}_2. \quad (2.13)$$

At the same time the form Eq.(2.4) of the average Green's function suggests that the main contribution to the momentum integration is given by momenta confined inside a ring of the radius  $p_F$  and the width  $1/\ell \ll p_F$  where  $\ell$  is the elastic mean free path  $\ell = v_F\tau$  [see Fig.4a]. The constraint Eq.(2.13) implies that not only  $\mathbf{p}$  but also  $-\mathbf{p} + \mathbf{p}_1 + \mathbf{p}_2 = \mathbf{p}'$  should be inside a narrow ring [see Fig.4b]. Thus



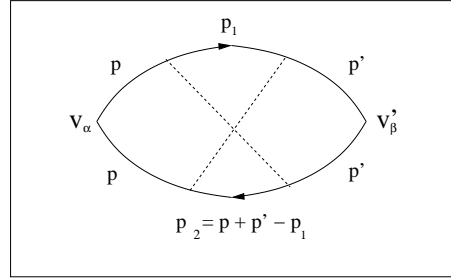


Fig. 3. The first of the "fan" diagrams.

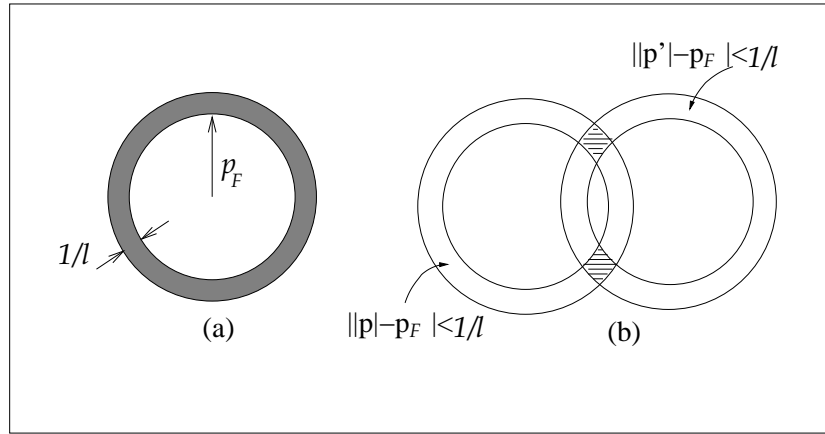


Fig. 4. Regions that make the main contribution to momentum integrals.

the effective region of  $\mathbf{p}$  integration is an *intersection* of two narrow rings which volume is reduced by a large factor of  $(p_F \ell)$  compared to an unconstrained case.

### 2.3. Weak localization correction.

The lesson one learns from the above example is that any intersection of dotted lines in systems with dimensionality greater than one brings about a small parameter  $1/(p_F \ell)$ . However this does not mean that all such diagrams should be neglected. As a matter of fact they contain an important new physics of *quantum coherence* that changes completely the behavior of low dimensional systems with  $d = 1, 2$  at small enough frequencies  $\omega$  leading to the phenomenon of Anderson localization.

For this to happen there should be something that compensates for the small

factor  $1/(p_F \ell)$ . We will see that this is a large return probability of a random walker or a particle randomly scattered off impurities in low-dimensional systems. On the formal level the corresponding diagrams are just the multiple scattering "fan" diagrams shown in Fig.5. One can see using the momentum con-

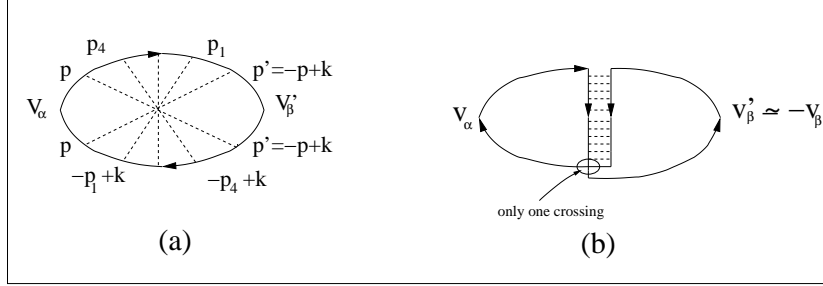


Fig. 5. Infinite series of "fan" diagrams.

servation that such diagrams have only one constraint of the type Eq.(2.13) independently of the number of dotted lines. This statement becomes especially clear if one rewrites the fan series in a form Fig.5b which contains a ladder series with all dotted lines parallel to each other and only one intersection of solid lines representing electron Green's functions. It is this ladder series called Cooperon which describes quantum interference that leads to Anderson localization.

To make connection between random walks (or diffusion) in space and a quantum correction to conductivity and to see how a compensation of the small parameter  $1/(p_F \ell)$  occurs we compute the Cooperon  $C(\mathbf{k}, \omega)$  for a small value of  $\mathbf{p}_1 + \mathbf{p}_2 = \mathbf{k}$  [see Fig.6.]. This series is nothing but a geometric progression with

$$C(\mathbf{k}, \omega) = \begin{array}{c} \xrightarrow{G_\varepsilon^R(\mathbf{p})} \\ \boxed{\phantom{p}} \\ \xleftarrow{G_{\varepsilon-\omega}^A(-\mathbf{p}+\mathbf{k})} \end{array} + \begin{array}{c} \xrightarrow{p} \quad \xrightarrow{p'} \\ \boxed{\phantom{p}} \quad \boxed{\phantom{p'}} \\ \xrightarrow{-p+k} \quad \xrightarrow{-p'+k} \end{array} + \dots$$

Fig. 6. Summation of the ladder series for a Cooperon.

the first term

$$\Pi_0 = \frac{1}{(2\pi\nu\tau)^2} \int d\mathbf{p} G_\varepsilon^R(\mathbf{p}) G_{\varepsilon-\omega}^A(-\mathbf{p} + \mathbf{k}) \quad (2.14)$$

and the denominator  $q = 2\pi\nu\tau\Pi_0$ . Thus we have

$$C(\mathbf{k}, \omega) = \frac{\Pi_0}{1 - q}. \quad (2.15)$$

To compute  $\Pi_0$  we write

$$\Pi_0 = \frac{\nu}{(2\pi\nu\tau)^2} \int d\mathbf{n} \int_{-\infty}^{+\infty} \frac{d\xi}{(\varepsilon - \xi + \frac{i}{2\tau})(\varepsilon - \omega - \xi + v_F \mathbf{n} \mathbf{k} - \frac{i}{2\tau})}. \quad (2.16)$$

In Eq.(2.16) we used an approximation  $\xi_{-\mathbf{p}+\mathbf{k}} \approx \xi_{\mathbf{p}} - v_F \mathbf{n} \mathbf{k}$  which is valid as long as  $|\mathbf{k}| \ll p_F$ . The pole integral in Eq.(2.16) can be done immediately with the result:

$$q = \int d\mathbf{n} \frac{1}{1 - i\omega\tau + i\ell \mathbf{n} \mathbf{k}}. \quad (2.17)$$

One can see a remarkable property of Eq.(2.17): the denominator of the geometric series Eq.(2.15) is equal to 1 in the limit  $\omega\tau, |\mathbf{k}|\ell \rightarrow 0$ . At finite but small  $\omega\tau, |\mathbf{k}|\ell \ll 1$  one can expand the denominator of Eq.(2.17) to obtain:

$$q \approx 1 + i\omega\tau - \ell^2 \mathbf{k}^2/d; \quad C(\mathbf{k}, \omega) \approx \frac{1}{2\pi\nu\tau^2} \frac{1}{D_0 \mathbf{k}^2 - i\omega}. \quad (2.18)$$

We immediately recognize an inverse diffusion operator in  $C(\mathbf{k}, \omega)$  which is divergent at small  $\omega$  and  $\mathbf{k}$ . This divergence is the cause of all the peculiar quantum-coherence phenomena in systems of dimensionality  $d \leq 2$ .

In particular the quantum correction to conductivity given by the diagram of Fig.5 can be written as:

$$\delta\sigma_{\alpha\beta} = \frac{\sigma^{(D)}}{2\pi\nu D_0} \times \frac{1}{Vol} \sum_{\mathbf{k}} \Gamma_{\alpha\beta} C(\mathbf{k}, \omega). \quad (2.19)$$

where  $\Gamma_{\alpha\beta}$  is the "Hikami box" shown in Fig.7: Its analytic expression is given by:

$$\int d\mathbf{p} \mathbf{v}_{\alpha}(\mathbf{p}) \mathbf{v}_{\beta}(-\mathbf{p}+\mathbf{k}) G_{\varepsilon}^R(\mathbf{p}) G_{\varepsilon-\omega}^A(\mathbf{p}) G_{\varepsilon}^R(-\mathbf{p}+\mathbf{k}) G_{\varepsilon-\omega}^A(-\mathbf{p}+\mathbf{k}). \quad (2.20)$$

In the limit  $\omega\tau \ll 1$  and  $|\mathbf{k}|\ell \ll 1$  one can set  $\omega = \mathbf{k} = 0$  in Eq.(2.20). Then  $\mathbf{v}(-\mathbf{p} + \mathbf{k}) = -\mathbf{v}(\mathbf{p}) = -\mathbf{v}_F \mathbf{n}$  and after the pole integration over  $\xi$  and the angular integration over  $\mathbf{n}$  we obtain for  $\Gamma_{\alpha\beta}$ :

$$- \int d\mathbf{n} v_F^2 \mathbf{n}_{\alpha} \mathbf{n}_{\beta} \int_{-\infty}^{+\infty} \frac{\nu d\xi}{(\varepsilon - \xi + \frac{i}{2\tau})^2 (\varepsilon - \xi - \frac{i}{2\tau})^2} = -4\pi\nu\tau^2 D_0. \quad (2.21)$$

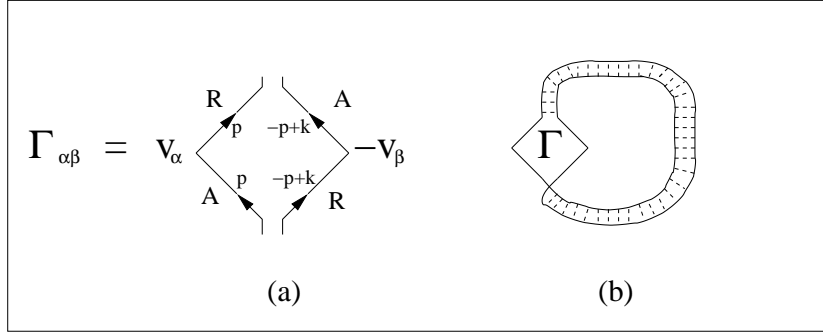


Fig. 7. The diagram representation for the Hikami box (a) and for the quantum correction to conductivity (b).

Finally using Eq.(2.19) we get:

$$\sigma(\omega) = \sigma^{(D)} \left( 1 - \frac{1}{\pi\nu} \frac{1}{Vol} \Re \sum_{\mathbf{k}} \frac{1}{D_0 \mathbf{k}^2 - i\omega} \right). \quad (2.22)$$

This is the celebrated formula for weak Anderson localization. One can see that the quantum correction is given by the sum over momenta of the diffusion propagator, that is, it is proportional to the *return probability* at a time  $\sim 1/\omega$  for a random walker in the  $d$ -dimensional space. A remarkable property of random walks in low-dimensional space is that the return probability increases with time. That is why the quantum correction to conductivity increases with decreasing the frequency  $\omega$  as  $1/\sqrt{\omega}$  in a quasi-one dimensional wire and as  $\log(1/\omega)$  in a two-dimensional disordered metal.

The structure of Eq.(2.22) suggests a qualitative picture of weak Anderson localization. It is an interference of two trajectories with a loop that differ only in the direction of traversing the loop [Fig.8]. Although the phase that corresponds to each trajectory is large and random, the phase *difference* between them is zero because of the time-reversal invariance. As a result they can interfere and amount to a creation of a *random standing wave* which is the paradigm of Anderson localization.

### 3. Non-linear response to a time-dependent perturbation

In this section we review the main steps of the Keldysh formalism [3, 4] which are necessary to describe a quantum system of non-interacting electrons subject to external time-dependent perturbation  $\hat{V}(t)$ .

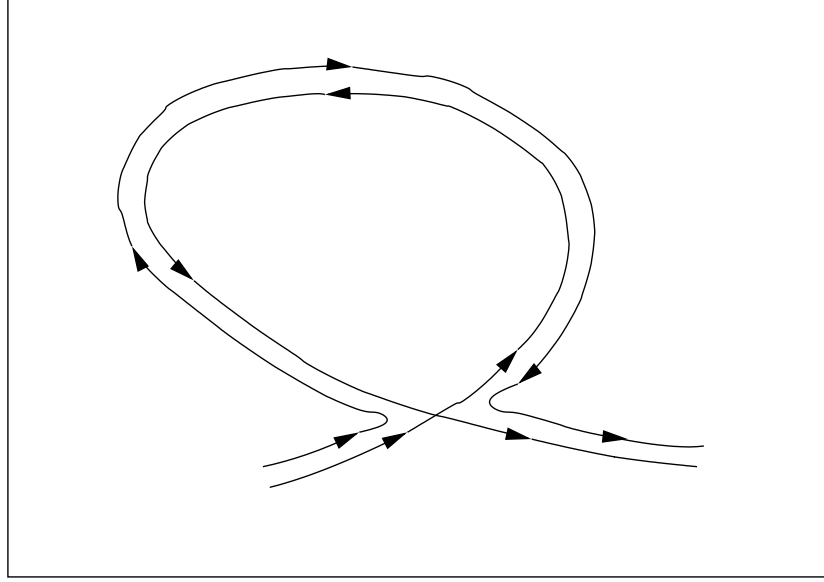


Fig. 8. Two interfering trajectories with loops

### 3.1. General structure of nonlinear response function.

The matrix Keldysh Green's function

$$\mathbf{G} = \begin{pmatrix} G^R & G^K \\ 0 & G^A \end{pmatrix} \quad (3.1)$$

contains – besides familiar retarded and advanced Green's functions  $\mathbf{G}^{11} = G^R$  and  $\mathbf{G}^{22} = G^A$  – also the third, Keldysh function  $\mathbf{G}^{12} = G^K$ . The latter is the only one needed to compute an expectation value of any operator  $\hat{O}$  both in equilibrium and beyond:

$$O = -iTr(\hat{O}G^K). \quad (3.2)$$

The retarded and advanced Green's functions appear only at the intermediate stage to make it possible to write down Dyson equations in the matrix form. It is of principal importance that the component  $\mathbf{G}^{21}$  is zero. One can show that this is a consequence of causality [5]. In equilibrium there is a relationship between  $G^K$  and  $G^{R/A}$ . It reads:

$$G_\epsilon^K = (G^R - G^A)_\epsilon \tanh\left(\frac{\epsilon}{2T}\right). \quad (3.3)$$

As without time-dependent perturbation the system is in equilibrium, the corresponding components  $G_{0,\varepsilon}^{R/A}$  and  $G_{0,\varepsilon}^K$  of the matrix Keldysh Green's function obey the relationship Eq.(3.3).

In the presence of the perturbation one can write the Dyson equation:

$$\mathbf{G} = \mathbf{G}_0 + \mathbf{G}_0 \hat{\mathbf{V}} \mathbf{G}, \quad (3.4)$$

where the operator of *external* time-dependent perturbation  $\hat{\mathbf{V}}(t)$  is proportional to a unit matrix in the Keldysh space. The structure of perturbation series for  $G^K$

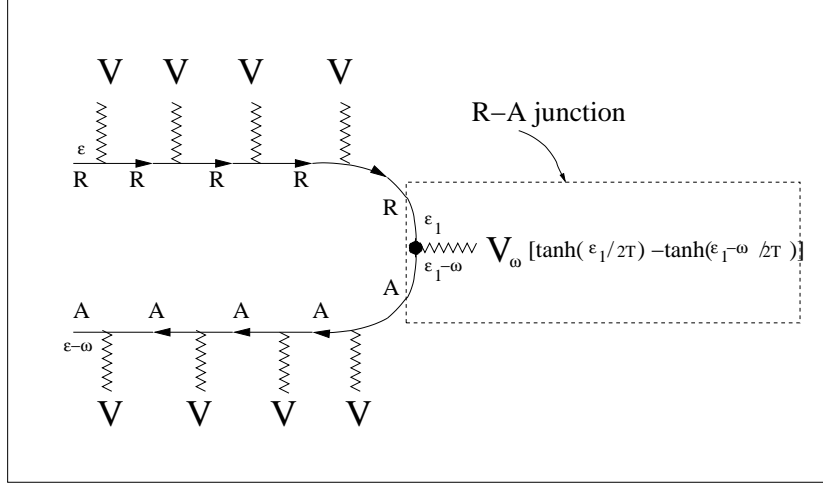


Fig. 9. The diagram representation of the "anomalous" term in the Keldysh function.

that corresponds to Eq.(3.4) is as follows:

$$G^K = G_0^{12} + G_0^{11} \hat{V} G_0^{12} + G_0^{12} \hat{V} G_0^{22} + G_0^{11} \hat{V} \dots G_0^{11} \hat{V} G_0^{12} \hat{V} G_0^{22} \dots G_0^{22} + \dots (3.5)$$

As  $G_0^{21} = 0$  and  $G_0^{12} = (G_0^R - G_0^A) \tanh(\varepsilon/2T)$  each term of the perturbation series Eq.(3.5) is a string of successive  $G_0^R$  functions followed by a string of  $G_0^A$  functions with only one switching point between them where the factor  $\tanh(\varepsilon/2T)$  is attached to. For the same reason the components  $G^R$  and  $G^A$  are the series that contain only  $G_0^R$  or  $G_0^A$ , respectively:

$$G^{R/A} = G_0^{R/A} + G_0^{R/A} \hat{V} G_0^{R/A} + G_0^{R/A} \hat{V} G_0^{R/A} \hat{V} G_0^{R/A} + \dots (3.6)$$

Using Eq.(3.6) one can replace the string of  $G_0^{R/A}$  functions in Eq.(3.5) by the exact retarded or advanced Green's function  $G_{\varepsilon,\varepsilon'}^{R/A}$  that depends on two energy

variables because of the breaking of translational invariance in the time domain by a time dependence of perturbation. The result is:

$$G_{\varepsilon, \varepsilon'}^K = G_{\varepsilon, \varepsilon'}^R \tanh\left(\frac{\varepsilon'}{2T}\right) - \tanh\left(\frac{\varepsilon}{2T}\right) G_{\varepsilon, \varepsilon'}^A + \int \frac{d\varepsilon_1}{2\pi} \int \frac{d\omega}{2\pi} G_{\varepsilon, \varepsilon_1}^R \hat{V}(\omega) G_{\varepsilon_1 - \omega, \varepsilon'}^A \left[ \tanh\left(\frac{\varepsilon_1}{2T}\right) - \tanh\left(\frac{\varepsilon_1 - \omega}{2T}\right) \right]. \quad (3.7)$$

The first two terms in Eq.(3.7) just reproduce the structure of the equilibrium Keldysh function Eq.(3.3). The most important for us will be the last, so called "anomalous" term  $G^{\text{anom}}$  in Eq.(3.7) as it contains both  $G_0^R$  and  $G_0^A$  functions which makes nonzero the pole integrals over  $\xi$  and allows to build a Cooperon. This term is graphically represented in Fig.9.

One can see that of all the vertices with a perturbation operator  $\hat{V}$  one is special: it is a switching point between the strings of retarded and advanced Green's functions, so called  $R-A$  junction [5]. It is convenient to switch from the energy to the time domain. In this representation the anomalous part of  $G^K$  reads [5]:

$$G_{t, t'}^{\text{anom}} = G_{t, t_1}^R G_{t_2, t'}^A (\hat{V}(t_2) - \hat{V}(t_1)) h_0(t_1 - t_2). \quad (3.8)$$

In Eq.(3.8) we denoted the Fourier transform of  $\tanh(\varepsilon/2T)$  as:

$$h_0(t) = \int \frac{d\varepsilon}{2\pi} e^{i\varepsilon t} \tanh(\varepsilon/2T) = \frac{iT}{\sinh(\pi T t)}. \quad (3.9)$$

We also assume integration over repeated time variables.

The graphic representation of Eq.(3.8) is given in Fig.10. Eqs.(3.7),(3.8) give a general structure of nonlinear response to a time-dependent perturbation. The main feature is the distinction between a regular  $\hat{V}$  vertex that connects two Green's functions with the same analytical properties (both  $G^R$  or both  $G^A$ ) and the  $R-A$  junction. One can see that the time variables do not match at the  $R-A$  junction because of the attached energy distribution function, while in at any regular vertex  $\hat{V}$  they do match.

### 3.2. Approximation of single photon absorption/emission

While an exact solution of the nonlinear response is a difficult task, there is an essentially nonlinear regime where a regular solution can be found. The corresponding approximation consists of expanding each *disorder averaged* retarded or advanced Green's function up to the second order in  $\hat{V}$ :

$$\langle G^{R/A} \rangle \approx \langle G_0^{R/A} \rangle + \langle G_0^{R/A} \rangle \hat{V} \langle G_0^{R/A} \rangle + \langle G_0^{R/A} \rangle \hat{V} \langle G_0^{R/A} \rangle \hat{V} \langle G_0^{R/A} \rangle \quad (3.10)$$

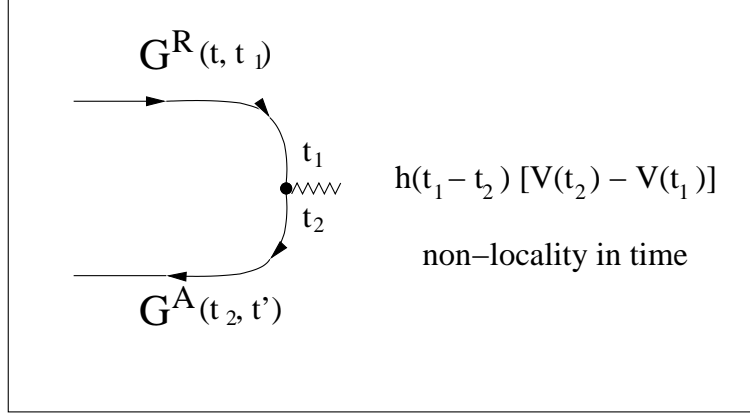


Fig. 10. Anomalous contribution to  $G^K$  in the time domain.

Yet, since the ladder series (a Cooperon) contains an *infinite* number of retarded (advanced) Green's functions, this approximation leads to an essentially non-linear results that do not reduce to a finite order response function. We will see that this approximation implies a *sequential* absorption/emission of photons rather than the *multiple-photon* processes.

Another approximation which is similar to  $\omega\tau \ll 1$  is based on the fact that the disorder average Green's function Eq.(2.4) decays exponentially in the time domain:

$$\langle G_0^{R/A} \rangle_t = \mp i \theta(\pm t) e^{-it\xi_P} e^{-t/\tau}. \quad (3.11)$$

Assuming that the momentum relaxation time is much shorter than the characteristic scale (e.g. the period) of a time-dependent perturbation one can approximate  $\langle G_0^{R/A} \rangle_t$  by a  $\delta$ -function and its derivative:

$$\langle G_0^{R/A} \rangle_t \approx \delta(t) \langle G_0^{R/A} \rangle_{\varepsilon=0} - i \partial_t \delta(t) \langle G_0^{R/A} \rangle_{\varepsilon=0}^2. \quad (3.12)$$

#### 4. Quantum rectification by a mesoscopic ring.

To proceed further on we need to make some assumptions about the time-dependent perturbation and specify an observable of interest.

In this section we consider a problem of rectification of an *ac signal* by a disordered metal. It has first been considered in Ref. [9] in a single-connected geometry where the entire effect is due to mesoscopic fluctuations. Here we



focus on the case of a quasi-one dimensional disordered metal ring pierced by a magnetic flux  $\phi(t)$  that contains both a constant part  $\phi$  and an oscillating part  $\phi_{ac}(t)$  [6–8]. In this case the topology of a ring and the presence of a constant magnetic flux makes it meaningful to study the *disorder-average* rectification effect.

The time-dependent perturbation in this case is:

$$\hat{V} = -\hat{v}_x \varphi(t), \quad \varphi(t) = \frac{2\pi}{L} \frac{\phi_{ac}(t)}{\phi_0}, \quad (4.1)$$

where  $L$  is the circumference of the ring, and  $\phi_0 = hc/e$  is the flux quantum. We assume that the ring curvature is large compared to all microscopic lengths in the problem so that it can be replaced by quasi-one dimensional wire along the  $x$ -axis with the twisted boundary conditions  $\Psi(L) = \Psi(0) \exp[2\pi i \phi / \phi_0]$ .

To solve this problem we need to take into account the ac perturbation only in the denominator  $q$  of the geometric series Eq.(2.15) that determines the Cooperon. This is because  $1 - q$  is governed by *small corrections* with the energy scale much smaller than  $1/\tau$ . The corrections due to the ac flux perturbation are given by the diagrams in Fig.11. Note that in linear in  $\hat{V}$  corrections one should take into account the small momentum  $\mathbf{k}$  whereas in quadratic in  $\hat{V}$  corrections  $\mathbf{k}$  can be set zero. All the corrections of Fig.11 can be computed by doing the pole integrals over  $\xi$  and angular integrals over  $\mathbf{n}$  as in the previous section. Note also that  $1 - q$  is essentially the *inverse* Cooperon operator. For an arbitrary time dependence of  $\varphi(t)$  one should replace  $-i\omega$  in Eq.(2.18) by the time derivative  $\partial_{t_1} - \partial_{t_2}$  which one can obtain from the second term in Eq.(3.12). Such a structure of the time derivatives implies that the sum of time arguments  $t_1 + t_2 = t'_1 + t'_2$  is conserved [see Fig.12] which is the consequence of the constant density of states approximation. As a result, the equation for a time-dependent Cooperon takes the form [5, 10, 11]:

$$\left\{ \frac{\partial}{\partial \eta} + \frac{D_0}{2} [\varphi(t + \eta/2) + \varphi(t - \eta/2) - \mathbf{k}_x]^2 \right\} C_t(\eta, \eta'; \mathbf{k}_x) = \frac{\delta(\eta - \eta')}{2\pi\nu\tau^2}, \quad (4.2)$$

where the momentum  $\mathbf{k}_x(\phi) = k_m(\phi) = (2\pi/L)(m - 2\phi/\phi_0)$  is quantized according to the twisted boundary conditions.

For completeness we give also an equation for the time-dependent *diffuson* [Fig.13]:

$$\left\{ \frac{\partial}{\partial t} + D_0 [\varphi(t + \eta/2) - \varphi(t - \eta/2) - \mathbf{k}_x]^2 \right\} D_\eta(t, t'; \mathbf{k}_x) = \frac{\delta(t - t')}{2\pi\nu\tau^2}, \quad (4.3)$$

where  $\mathbf{k}_x = (2\pi/L) m$  is independent of the DC flux  $\phi$ .

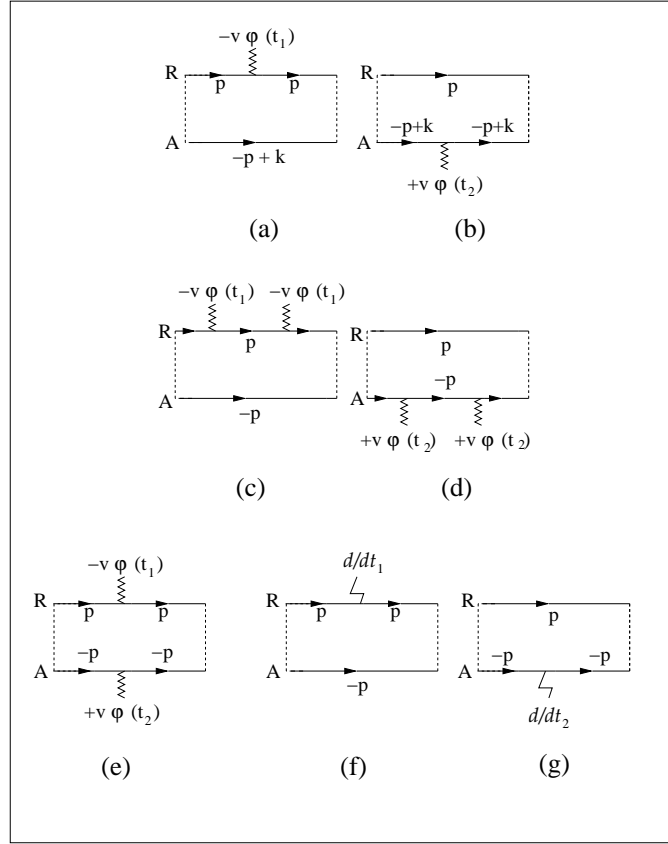


Fig. 11. The ac flux and time-derivative corrections to the inverse Cooperon operator.

In this case the structure of the time-derivative  $\partial_{t_1} + \partial_{t_2}$  suggests that the *difference* of the time arguments is conserved  $t_1 - t_2 = t'_1 - t'_2$ .

In general the current response  $I(t)$  to the electric field  $E(t - \tau)$  is given by:

$$I(t) = \int_0^\infty K(t, \tau) E(t - \tau) d\tau, \quad (4.4)$$

where in our particular case  $E(t) = -\partial_t \varphi(t)$ .

At small  $1/p_F \ell$  the main contribution to the *nonlinear* response function is that of the quantum coherence correction shown in Figs.5,7. All what we have to do in order to compute this nonlinear response function is to substitute the time-dependent Cooperon into Eq.(2.19) and take care of all the time arguments [see

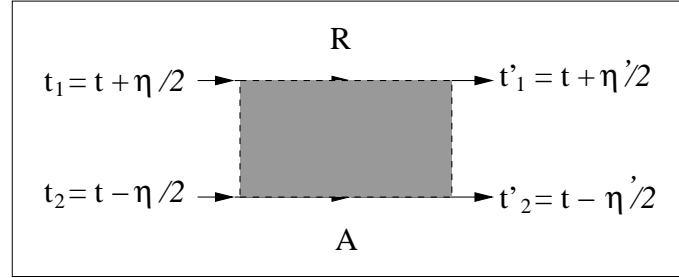


Fig. 12. The time arguments in the Cooperon.

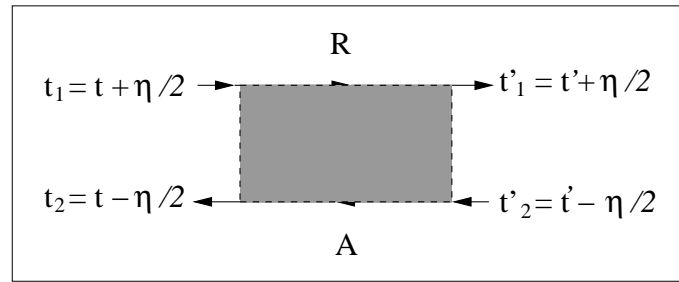


Fig. 13. The time-dependent Diffuson.

Fig.14]. Namely, (i) according to Eq.(3.12) the time arguments corresponding to the beginning and the end of any solid line representing the disorder averaged functions  $\langle G_0^{R/A} \rangle$  should be the same and (ii) the sum (difference) of "incoming times" in the Cooperon (Diffuson) are equal to the sum (difference) of "outgoing times" as in Figs.12,13. Note that application of rules (i),(ii) to the diagram of Fig.14 leads to the coinciding time arguments  $t_1 \rightarrow t_2 = t - \tau$  in the corresponding retarded-advanced junction (see Fig.10). This ensures fulfillment of Eq.(4.4), as  $h_0(t_1 - t_2)(V(t_2) - V(t_1)) \rightarrow v_x \partial_t \varphi(t - \tau) \propto E(t - \tau)$ .

The disorder average current response function  $K(t, \tau)$  is equal to:

$$K(t, \tau) = \sigma^D \tau^{-1} e^{-t/\tau} - \frac{4e^2 D_0}{h} \tilde{C}_{t-\tau/2}(\tau, -\tau), \quad (4.5)$$

where  $\tilde{C}_t(\eta, \eta') = (2\pi\nu\tau^2/Vol) \sum_{\mathbf{k}_x} C_t(\eta, \eta'; \mathbf{k}_x)$  and  $C_t(\eta, \eta'; \mathbf{k}_x)$  is the solution to Eq.(4.2):

$$2\pi\nu\tau^2 C_t(\eta, \eta'; \mathbf{k}_x) = \theta(\eta - \eta') \times \quad (4.6)$$

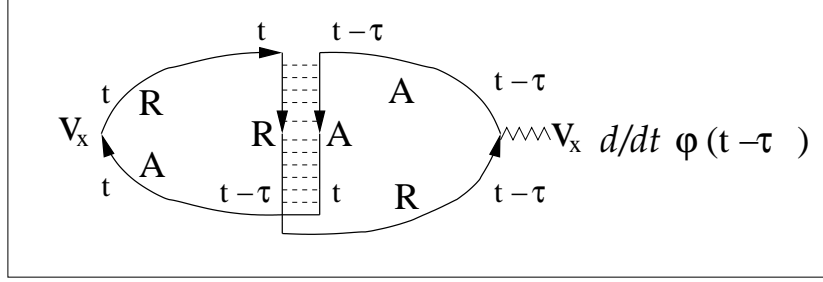


Fig. 14. Nonlinear current response function and the Cooperon.

$$\exp \left\{ -\frac{D_0}{2} \int_{\eta'}^{\eta} [\varphi(t + \zeta/2) + \varphi(t - \zeta/2) - \mathbf{k}_x]^2 d\zeta \right\}.$$

The first term in Eq.(4.5) is just the linear response given by the diagrams Fig.1c,d. The second term corresponds to the quantum-coherent contribution of Fig.14. The fact that  $\tilde{C}_{t-\tau/2}(\tau, -\tau)$  depends not only on  $\tau$  but also on  $t$  makes it possible to have dc response caused by ac electric field  $E(t) = -\partial_t \varphi(t)$ .

For a particular case of a ring with a constant and an *ac* magnetic flux we note that the *dc* response arises only from *odd* terms of expansion of Eq.(4.6) in powers of the ac perturbation  $\varphi(t)$ . As odd terms in  $\varphi(t)$  enter in a combination  $\varphi(t)\mathbf{k}_x$  the *dc* response involves only *odd* terms in  $\mathbf{k}_x = k_m = (2\pi/L)(m - 2\phi/\phi_0)$ . If the constant magnetic flux  $\phi = 0$  or we neglect quantization of momentum and do an integral over  $\mathbf{k}_x$  instead of a sum, the result for the odd in  $\varphi(t)$  part of  $\tilde{C}_t(\eta, \eta')$  is zero. Otherwise it is *periodic* in the flux  $\phi$  with the period  $\phi_0/2$ , since  $k_m(\phi + \phi_0/2) = k_{m-1}(\phi)$  and the summation is over all integer  $m$ . We see that the dc response to the ac perturbation, or the rectification of the ac flux by an ensemble of mesoscopic rings, is an essentially quantum, Bohm-Aharonov-like effect. Furthermore, it is an *odd* in the flux Bohm-Aharonov effect that can be represented by the Fourier series:

$$\langle I_{dc}(\phi) \rangle = \sum_{n=1}^{\infty} I_n \sin \left( \frac{4\pi n \phi}{\phi_0} \right). \quad (4.7)$$

Expression Eq.(4.7) has the same symmetry and periodicity in the magnetic flux  $\phi$  as the disorder-averaged equilibrium persistent current [12, 13]. However, its magnitude may be much larger (in the grand-canonical ensemble considered here the disorder-averaged persistent current is strictly zero).

Applying the Poisson summation trick

$$\begin{aligned} \sum_m f(m - \phi) &= \int dx f(x - \phi) \sum_m \delta(x - m) = \\ &= \int dx f(x - \phi) \sum_n e^{2\pi i n x} = \sum_n e^{2\pi i n \phi} \int dx e^{2\pi i n x} f(x) \end{aligned} \quad (4.8)$$

to Eq.(4.6) one obtains

$$I_n = \frac{4ieD_0}{\pi L} \int_0^\infty d\tau \overline{C_t^{(n)}(\tau) \partial_t \varphi(t - \tau/2)}, \quad (4.9)$$

where the overline means averaging over time  $t$  and

$$C_t^{(n)}(\tau) = \sqrt{\frac{\tau_D}{4\pi\tau}} e^{-\frac{n^2\tau_D}{4\tau}} e^{inS_1[\varphi]} e^{-\tau S_2[\varphi]}. \quad (4.10)$$

Here  $\tau_D = L^2/D_0$  is time it takes for a diffusing particle to go around the ring, and  $S_{1,2}$  are defined as follows:

$$S_1[\varphi] = 2L \left[ \frac{1}{\tau} \int_{t-\tau/2}^{t+\tau/2} \varphi(t_1) dt_1 \right] \equiv 2L \langle \varphi_{t_1} \rangle_{t;\tau}, \quad (4.11)$$

$$S_2[\varphi] = 2D_0 [\langle \varphi_{t_1}^2 \rangle_{t;\tau} + \langle \varphi_{t_1} \varphi_{2t-t_1} \rangle_{t;\tau} - 2\langle \varphi_{t_1} \rangle_{t;\tau}^2]. \quad (4.12)$$

Eqs.(4.10)-(4.12) are valid for an arbitrary time-dependence of  $\varphi(t)$ . However, they take the simplest form for a noise-like ac flux with the small correlation time  $\tau_0 \ll \tau_D$  (but we assume  $\tau_0 \gg \tau$ ). In this case the second and the third terms in Eq.(4.12) can be neglected and the first term reduces to a *constant* that determines the *dephasing time* caused by ac noise:

$$\frac{1}{\tau_\varphi} = 2D_0 \overline{\varphi^2(t)}. \quad (4.13)$$

Then the time averaging in Eq.(4.9) reduces to

$$\overline{-i\partial_t \varphi(t - \tau/2) \exp \left\{ \frac{in}{\tau} 2L \int_{t-\tau/2}^{t+\tau/2} \varphi(t_1) dt_1 \right\}} = \frac{n}{\tau} 2L \overline{\varphi^2(t)}. \quad (4.14)$$

Since the time-average of the a total time-derivative is zero, we can transfer the differentiation to the exponent. For the case of a white-noise ac flux only the

lower limit of integration in the exponent should be differentiated, the quantity  $\langle \varphi_{t_1} \rangle_{t;\tau}$  being set zero afterwards. The remaining integral over  $\tau$  is done exactly:

$$\int_0^\infty \frac{d\tau}{\tau^{3/2}} \exp \left[ -\frac{n^2 \tau_D}{4\tau} - \frac{\tau}{\tau_\varphi} \right] = \frac{2\sqrt{\pi}}{n\sqrt{\tau_D}} e^{-n\sqrt{\tau_D/\tau_\varphi}} \quad (4.15)$$

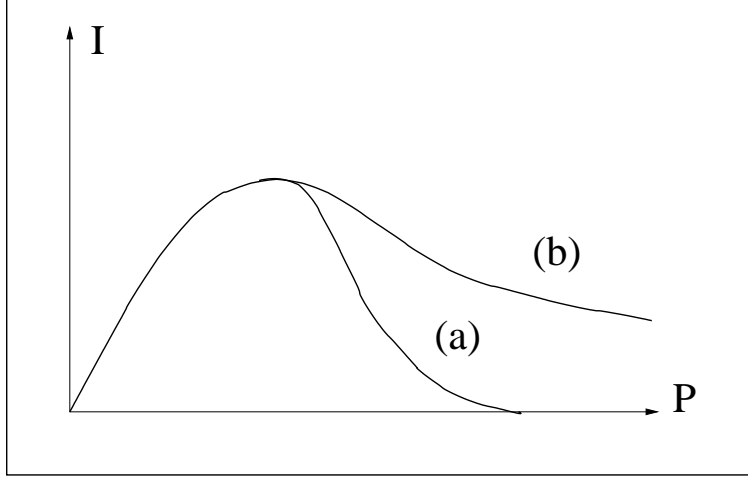


Fig. 15. The dependence of  $I_1$  on the ac power  $P = \overline{\varphi^2(t)}$  for a white-noise (a) and harmonic (b) perturbation.

Finally we arrive at a remarkably simple result for the disorder-average dc current generated in mesoscopic rings by a white-noise ac perturbation [8]:

$$I_n = -\frac{4}{\pi} \left( \frac{e}{\tau_\varphi} \right) \exp \left[ -n \frac{L}{L_\varphi} \right], \quad (4.16)$$

where the *dephasing length* is equal to:

$$\frac{1}{L_\varphi^2} = \frac{1}{D_0 \tau_\varphi} = 2 \overline{\varphi^2(t)} \quad (4.17)$$

It follows from Eq.(4.16) that the weak ac white noise produces a net dc current in an ensemble of mesoscopic rings which is of the order of  $e/\tau_\varphi$  where  $\tau_\varphi$  is the dephasing time produced by the same ac noise. At an ac power large enough to produce a dephasing length smaller than the circumference of a ring times the winding number  $n$ , the destructive effect of ac perturbation prevails and the current  $I_n$  decreases exponentially [see Fig.15].

Note that the tail of the dependence  $I_n$  on the ac power is very sensitive to the correlations in the ac perturbation at different times. For instance, in the case of harmonic perturbation where  $\varphi(t)$  has an infinite range time-correlations, the current decreases very slowly, only as the inverse square-root of the ac power [6]. We will see later on that this is related with the phenomenon of *no-dephasing points*.

## 5. Diffusion in the energy space.

In this section we apply the Keldysh formalism outlined above to the problem of *heating* by external time-dependent perturbation. The main object to study will be the *non-equilibrium* electron energy distribution function:

$$f(\varepsilon; t) = \frac{1}{2} - \frac{1}{2} \int d\eta \, h_t(\eta) e^{-i\varepsilon\eta} \quad (5.1)$$

which is related to the Keldysh function  $G^K(t, t') \equiv Vol^{-1} \int d^d \mathbf{r} \, G^K(t, t'; \mathbf{r}, \mathbf{r})$  at coincident space variables (averaged over volume):

$$G^K(t + \eta/2, t - \eta/2) = -2\pi i \nu h_t(\eta). \quad (5.2)$$

Eqs.(5.1),(5.2) generalize Eq.(3.3) to the case of non-equilibrium, time-dependent energy distribution function. The total energy  $\mathcal{E}(t)$  of electron system can be expressed in terms of  $f(\varepsilon, t)$ :

$$\mathcal{E}(t) = \nu \, Vol \int d\varepsilon \, \varepsilon [f(\varepsilon, t) - \theta(-\varepsilon)] + const. \quad (5.3)$$

Then the time-dependent *absorption rate*  $W(t) = \partial_t \mathcal{E}(t)$  is given by:

$$W(t) = -\frac{Vol}{2} \lim_{\eta \rightarrow 0} \partial_t \partial_\eta G^K \left( t + \frac{\eta}{2}, t - \frac{\eta}{2} \right) = \frac{i\pi}{\delta} \lim_{\eta \rightarrow 0} \partial_t \partial_\eta h_t(\eta), \quad (5.4)$$

where  $\delta = (\nu \, Vol)^{-1}$  is the mean separation between electron energy levels (mean level spacing).

For tutorial reasons in this section we consider a specific model system described by the Hamiltonian:

$$\hat{H} = \varepsilon(\hat{\mathbf{p}}) + U(\mathbf{r}) + V(\mathbf{r}) \varphi(t), \quad (5.5)$$

where not only  $U(\mathbf{r})$  given by Eq.(2.11) but also the perturbation potential  $V(\mathbf{r})$  is a Gaussian random field which is statistically independent of  $U(\mathbf{r})$  and is described by the correlation function:

$$\langle V(\mathbf{r}) V(\mathbf{r}') \rangle = \frac{\Gamma}{\pi \nu} \delta(\mathbf{r} - \mathbf{r}'). \quad (5.6)$$

This model is the simplest example of a *potential ac source* in contrast to the *flux ac source* considered in the previous section. In the low-frequency  $\omega\tau_D \ll 1$  and the modestly low ac intensity  $\Gamma\tau \ll 1$  limits this model is equivalent to the *random matrix theory* with the time-dependent Hamiltonian [5, 11]:

$$\hat{H}_{RMT} = \hat{H}_0 + \hat{V} \varphi(t), \quad (5.7)$$

where both  $\hat{H}_0$  and  $\hat{V}$  are random real-symmetric  $N \times N$  matrices from the independent Gaussian Orthogonal Ensembles described by the correlation functions  $\langle (H_0)_{nm} \rangle = \langle V_{nm} \rangle = 0$ :

$$\begin{aligned} \langle (H_0)_{nm} (H_0)_{n'm'} \rangle &= N(\delta/\pi)^2 [\delta_{nn'}\delta_{mm'} + \delta_{nm'}\delta_{mn'}], \\ \langle V_{nm} V_{n'm'} \rangle &= (\Gamma\delta/\pi) [\delta_{nn'}\delta_{mm'} + \delta_{nm'}\delta_{mn'}], \end{aligned} \quad (5.8)$$

with  $\delta = 1/(\nu Vol)$  being the mean level spacing.

In this RMT limit *all* the disordered and chaotic systems described by a real, spin-rotational invariant Hamiltonian are believed to have a universal behavior in the limit  $L, N \rightarrow \infty$  which is characterized by only two parameters  $\delta$  and  $\Gamma$  and one dimensionless function  $\varphi(t)$ .

Let us first consider the disorder-averaged  $G^K$  in the non-crossing approximation. Since there are no vector vertices in the present model, the ladder diagrams (Lose Diffuson) similar to Fig.2 make the main contribution. The corresponding diagrams are shown in Fig.16 where the wavy line describes the  $\langle VV \rangle$  correlator, Eq.(5.6). The condition

$$\Gamma\tau \ll 1 \quad (5.9)$$

allows to keep only the linear in  $\hat{V}$  term in the expansion Eq.(3.10) for the  $\langle G^{R/A} \rangle$  function attached to the RA-junction. Note that the diagrams Fig.16a,b have opposite signs because  $\int d\xi (\xi \pm i/2\tau)^{-1} = \mp\pi i$ . The result of calculation of both diagrams is:

$$\begin{aligned} \delta G^K &= (2\pi\nu\tau)^2 (i\pi\nu)(\Gamma/\pi\nu) D_\eta(t, t') \\ &\times [\varphi(t' + \eta/2) - \varphi(t' - \eta/2)]^2 h_0(\eta). \end{aligned} \quad (5.10)$$

so that

$$h_t(\eta) = \left(1 - \tilde{D}_\eta(t, t') \Gamma [\varphi(t' + \eta/2) - \varphi(t' - \eta/2)]^2\right) h_0(\eta), \quad (5.11)$$

where the integration over  $t'$  is assumed;  $h_0(\eta)$  is determined by Eq.(3.9), and  $\tilde{D}_\eta(t, t') = 2\pi\nu\tau^2 D_\eta(t, t'; \mathbf{k} = 0)$  is given by Eq.(4.3) with  $D_0 \rightarrow \Gamma$ . One can check using this equation that  $h_t(\eta)$  obeys the equation:

$$\left\{ \partial_t + \Gamma [\varphi(t + \eta/2) - \varphi(t - \eta/2)]^2 \right\} h_t(\eta) = 0. \quad (5.12)$$



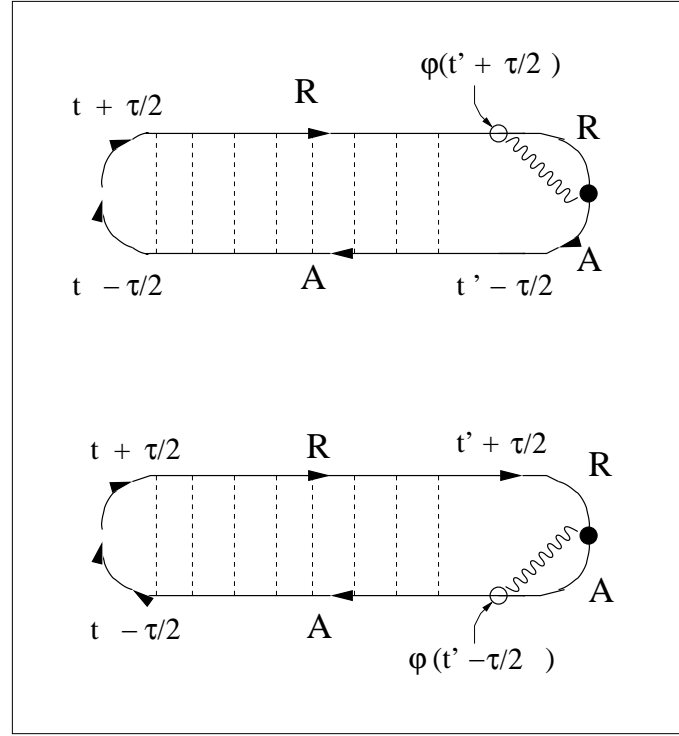


Fig. 16. The Loose Diffusion diagrams for the absorption rate: the dotted lines represent the  $\langle UU \rangle$  correlation function while the wavy line corresponds to the  $\langle VV \rangle$  correlator.

This allows to give an explicit solution for  $h_t(\eta)$ :

$$h_t(\eta) = h_0(\eta) \exp \left\{ -\Gamma \int_0^t [\varphi(\zeta + \eta/2) - \varphi(\zeta - \eta/2)]^2 d\zeta \right\} \quad (5.13)$$

Note that a nontrivial dynamics of  $h_t(\eta)$  and thus that of  $f(\varepsilon; t)$  is hidden in the exponential factor which is a purely classical object. The Fermi statistics of electrons considered here is taken into account by an initial distribution  $h_0(\eta)$ . At  $\eta\omega \ll 1$  where  $\omega$  is the typical frequency of oscillations in  $\varphi(t)$ , or equivalently at the energy resolution  $\delta\varepsilon \gg \omega$ , one can approximate  $\varphi(\zeta + \eta/2) - \varphi(\zeta - \eta/2) \approx (\partial_t \varphi) \eta$ . Then the exponent in Eq.(5.13) reduces to  $\exp \left[ -t \Gamma \overline{(\partial_t \varphi)^2} \eta^2 \right]$  which corresponds to Eq.(5.12) of the form:

$$\{ \partial_t + D_E \eta^2 \} h_t(\eta) = 0, \quad \{ \partial_t - D_E \partial_\varepsilon^2 \} f(\varepsilon, t) = 0. \quad (5.14)$$

In this approximation we come to the diffusion equation for the energy distribution function with the energy diffusion coefficient:

$$D_E = \Gamma \overline{(\partial_t \varphi)^2} \sim \Gamma \omega^2. \quad (5.15)$$

For a harmonic perturbation  $\varphi(t) = \cos(\omega t)$  the form of energy diffusion coefficient allows a simple interpretation. This is a random walk in the energy space due to a sequential absorption or emission of photons with the energy  $\hbar\omega$ . Then the size of an elementary step is  $\pm\hbar\omega$  and the rate of making steps is  $\Gamma/\hbar$ . Now it is clear that the condition Eq.(5.9) that allows to use the approximation Eq.(3.10) has a physical meaning of a condition to absorb/emit *at most* one photon during the time of elastic mean free path. The opposite condition would mean that many photons can be absorbed/emitted during the time  $\tau$  which implies inelastic processes being stronger than the elastic ones.

Using the diffusion equation we express  $\partial_t h_t(\eta) = -D_E \eta^2 h_t(\eta)$ . Then Eq.(5.4) gives for the net absorption rate:

$$W(t) = -i\pi (D_E/\delta) \lim_{\eta \rightarrow 0} \partial_\eta (\eta^2 h_t(\eta)). \quad (5.16)$$

It is important that

$$h_t \approx \frac{i}{\pi\eta}, \quad \eta \rightarrow 0. \quad (5.17)$$

for all  $h_t(\eta)$  corresponding to the Fermi-like energy distribution function  $f(\varepsilon; t) < 1$  with  $f(\varepsilon \rightarrow +\infty; t) = 0$ ,  $f(\varepsilon \rightarrow -\infty; t) = 1$ . Thus the existence of the Fermi sea makes the net absorption rate non-zero despite the diffusion character of the energy distribution dynamics:

$$W(t) = W_0 = \frac{D_E}{\delta}. \quad (5.18)$$

## 6. Quantum correction to absorption rate.

We see that the non-crossing, or zero-loop, approximation leads to the classical picture of a time-independent absorption rate, the so called *Ohmic absorption*. This is in line with the fact established below that the same approximation leads to the classical Drude conductivity. Let us go beyond and consider the diagrams for  $G^K$  that contain one crossing or one Cooperon loop. Different ways of presenting such a diagram are shown in Fig.17. This is essentially the same fan diagram with the Loose Diffuson attached to it. However, because the perturbation does not contain a vector vertex, one should take a special care about the

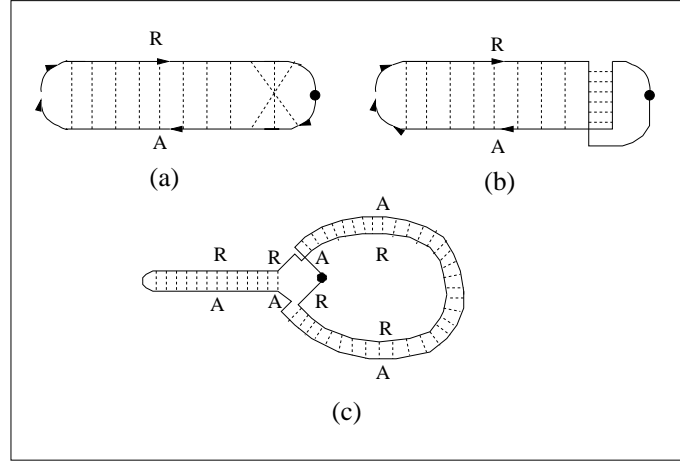


Fig. 17. Diagrams for weak dynamic localization.

Hikami box. It is shown in Fig.18. Here a new element – besides the correlation between two  $\hat{V}$  vertices that first appeared in Fig.16– is the dotted line installed between two retarded or two advanced Green's functions. The rules of such an installation are (i) non-crossing of dotted-dotted and dotted-wavy lines and (ii) the presence of both retarded and advanced functions in each "cell" separated by dotted or wavy lines (otherwise the  $\xi$ -integral zero). One can see that the sum of three diagrams in Fig.18a-c and in Fig.18d-f are zero. The remaining diagrams Fig.18g and Fig.18h have opposite signs so that the R-A junction and the  $\hat{V}(t)$  vertices (denoted by an open circle in Fig.18) that appear as the first term of expansion of  $\langle G^{R/A} \rangle$  compose a combination

$$\begin{aligned} & \Gamma \left( \varphi(t' + \eta/2) - \varphi(t' - \eta/2) \right) \left( \varphi(t' - t_1) - \varphi(t' - t_1 - \eta) \right) h_0(\eta) \\ & \approx \Gamma \partial_{t'} \varphi(t') \partial_{t'} \varphi(t' - t_1) \eta^2 h_0(\eta). \end{aligned} \quad (6.1)$$

The contribution to the absorption rate that comes from the diagram of Fig.17 is computed with the help of Eq.(5.4). The limit  $\lim_{\eta \rightarrow 0} \partial_{\eta} \eta^2 h_0(\eta)$  results in a universal constant  $i/\pi$ , and the time derivative  $\partial_t$  of the Loose Diffuson gives a  $\delta(t - t')$  function in the leading order in  $\hat{V}$ . So we obtain a quantum correction to the absorption rate [14]:

$$\frac{\delta W(t)}{W_0} = \frac{\Gamma \delta}{\pi D_E} \int_0^t \partial_t \varphi(t) \partial_t \varphi(t - t_1) \tilde{C}_{t-t_1/2}(t_1, -t_1) dt_1. \quad (6.2)$$

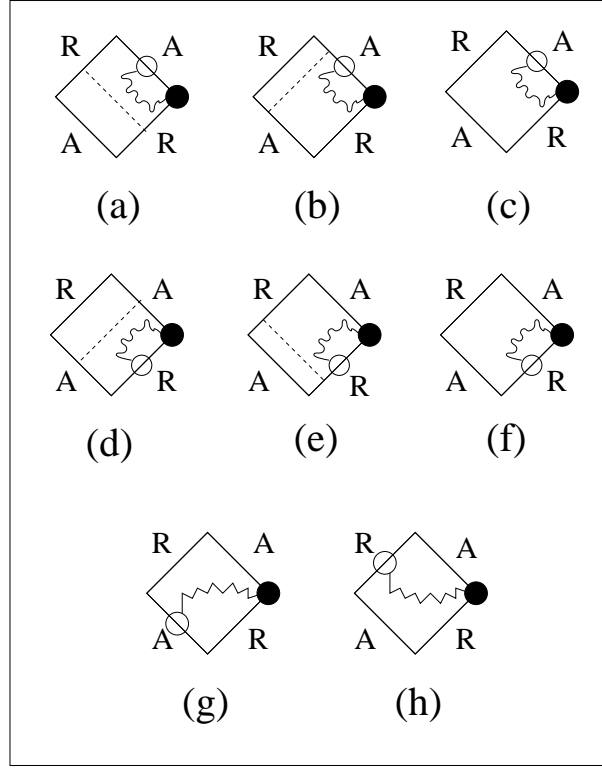


Fig. 18. Hikami box for a scalar vertex.

where the limits of integration are fixed by an assumption that a time-dependent perturbation has been switched on at  $t = 0$ ;  $C_t(\eta, \eta'; \mathbf{k})$  is the Cooperon, and

$$\tilde{C}_t(\eta, \eta') = (2\pi\nu\tau^2) \frac{1}{Vol} \sum_{\mathbf{k}} C_t(\eta, \eta'; \mathbf{k}). \quad (6.3)$$

Here we have to make some remarks. Eq.(6.2) is general and gives the first quantum correction to the absorption rate in a disordered or chaotic system of any geometry. However, the quantity  $\tilde{C}_t(\eta, \eta')$  depends on the type of perturbation and on the system geometry. For a closed system of finite volume  $Vol$  there always exists a regime where geometry of the system does not play any role. This is the limit where the typical frequency  $\omega$  of perturbation is much smaller than the so called Thouless energy  $E_{Th}$ . In disordered systems with the diffusion character of electron transport, the Thouless energy coincides with the gap between the

*zero diffusion mode* that corresponds to  $\mathbf{k} = 0$  and the first mode of dimensional quantization that corresponds to  $k \sim 2\pi/L$ , where  $L$  is the *largest* of the system sizes. In this case it is of the order of the inverse diffusion time  $E_{Th} \sim 1/\tau_D$ . For such small frequencies one can neglect the higher modes with nonzero values of  $\mathbf{k}$  and consider the zero diffusion mode with  $\mathbf{k} = 0$  that always exists in closed systems. In this *zero-mode*, or *ergodic* limit the actual shape of the system does not matter at all. One can show that this is exactly the limit where the results obtained using the Hamiltonian Eq.(5.5) are equivalent to the results obtained starting from the random matrix theory Eq.(5.7).

However, even in the ergodic limit the results for the Cooperon depend on the *topology* of the system. The equation for the Cooperon Eq.(4.2) that corresponds to the *non-single connected* topology of a ring and a *global vector-potential* perturbation differs from that for the scalar potential perturbations with local correlations in space described by Eqs.(5.5),(5.6).

To see the difference we re-derive the Cooperon for the case of a scalar potential perturbation. The corresponding diagrams analogous to those shown in Fig.11 for the case of the global vector-potential perturbation are given in Fig.19. As a result of calculation of the corresponding  $\xi$ -integrals we obtain an equation

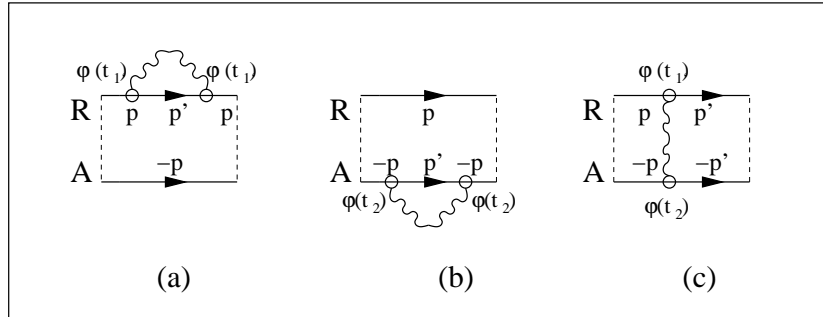


Fig. 19. The ac scalar potential corrections to the inverse Cooperon.

(in the ergodic limit  $\mathbf{k}=0$ ):

$$\left\{ 2 \frac{\partial}{\partial \eta} + \Gamma [\varphi(t + \eta/2) - \varphi(t - \eta/2)]^2 \right\} \tilde{C}_t(\eta, \eta') = 2\delta(\eta - \eta'). \quad (6.4)$$

This equation contains the *difference*  $\varphi(t + \eta/2) - \varphi(t - \eta/2)$  instead of the sum in Eq.(4.2). One can show [5] that the time-dependent random matrix theory that reproduces the Cooperon with the sum  $\varphi(t + \eta/2) + \varphi(t - \eta/2)$  corresponds to the random perturbation matrix  $\hat{V}$  which is pure imaginary *anti*-symmetric, rather than the real symmetric as in Eq.(5.7).

The corresponding equation for a time-dependent Diffuson appears to be the same as Eq.(4.3):

$$\left\{ \frac{\partial}{\partial t} + \Gamma [\varphi(t + \eta/2) - \varphi(t - \eta/2)]^2 \right\} \tilde{D}_\eta(t, t') = \delta(t - t'). \quad (6.5)$$

To complete the solution Eq.(6.2) we give a solution to Eq.(6.4) which is valid for an *arbitrary* time dependence of  $\varphi(t)$ :

$$\tilde{C}_t(\eta, \eta') = \theta(\eta - \eta') \exp \left\{ -\frac{\Gamma}{2} \int_{\eta'}^{\eta} [\varphi(t + \zeta/2) - \varphi(t - \zeta/2)]^2 d\zeta \right\}. \quad (6.6)$$

## 7. Weak dynamic localization and no-dephasing points.

In this section we concentrate on the *oscillating* time dependence of perturbation with  $\overline{\varphi(t)} = 0$  and  $\overline{\varphi^2(t)} = 1$ . The simplest example is that of a *white-noise* with  $\overline{\varphi(t)\varphi(t')} = 0$  for  $t \neq t'$ . Then Eq.(6.6) takes the form:

$$\tilde{C}_t(\eta, \eta') = \theta(\eta - \eta') \exp [-\Gamma (\eta - \eta')]. \quad (7.1)$$

The negative exponential factor describes *dephasing* by a white noise perturbation. Because of the factor  $\partial_t \varphi(t) \partial_{t'} \varphi(t - t_1)$  the effective range of integration in Eq.(6.2) is of the order of the correlation time  $\tau_0 \ll 1/\Gamma$ . This makes the correction to the absorption rate vanishing  $\delta W(t)/W_0 \rightarrow 0$  in the white-noise limit  $\tau_0 \rightarrow 0$ .

Now let us consider the simplest example of an *infinite-range* time correlations. This is the case of a harmonic perturbation  $\varphi(t) = \cos(\omega t)$ . Then for  $\omega|\eta - \eta'| \gg 1$  the Cooperon takes again the form Eq.(7.1) but with the *time-dependent* dephasing rate:

$$\Gamma_t = \Gamma \sin^2 \omega t \quad (7.2)$$

One can see that there are certain moments of time  $\omega t_n = \pi n$  ( $n = \text{integer}$ ) where the dephasing rate is zero. We will refer to these points  $t_n$  as *no-dephasing* points [15].

This remarkable phenomenon is generic to harmonic perturbation and is also present for the case of an ac vector-potential considered in the previous section. Its physical meaning is quite simple. Consider again a pair of electron trajectories with a closed loop shown in Fig.8. In the presence of a time-dependent vector-potential  $\mathbf{A}(t)$  the phase difference between these two trajectories is no longer zero but a random quantity:

$$\delta\Phi = \int_0^\tau \mathbf{A}(t') [\mathbf{v}_1(t') - \mathbf{v}_2(t')] dt', \quad (7.3)$$

where  $\mathbf{v}_{1,2}(t)$  are electron velocities at a time  $t$  and  $\mathcal{T}$  is the time it takes for an electron to make a loop (the traversing time). For loops with the opposite directions of traversing  $\mathbf{v}_1(t') = -\mathbf{v}_2(\mathcal{T} - t')$  [see Fig.20]. Then we obtain

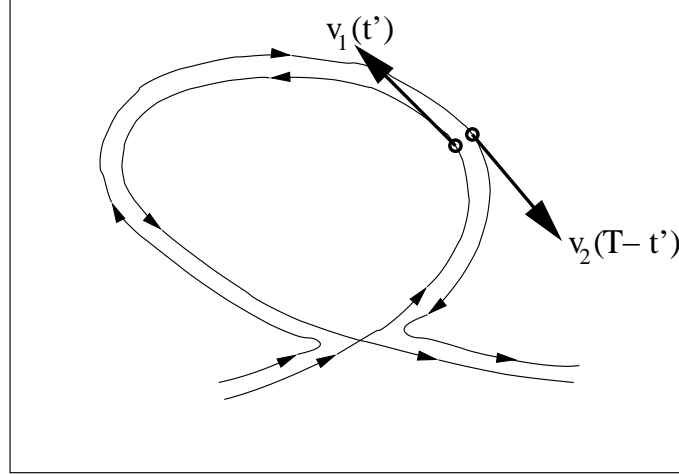


Fig. 20. Trajectories with loops traversed in opposite directions and synchronization.

$$\delta\Phi = \int_{-\mathcal{T}/2}^{\mathcal{T}/2} [\mathbf{A}(\mathcal{T}/2 + t') + \mathbf{A}(\mathcal{T}/2 - t')] \mathbf{v}_1(t' + \mathcal{T}/2) dt' \quad (7.4)$$

Now assuming the period of oscillations of  $\mathbf{A}(t)$  to be large compared to the velocity correlation time  $\tau$  we obtain after averaging over  $\mathbf{v}_1$ :

$$\langle (\delta\Phi)^2 \rangle = D_0 \int_{-\mathcal{T}/2}^{\mathcal{T}/2} [\mathbf{A}(\mathcal{T}/2 + t') + \mathbf{A}(\mathcal{T}/2 - t')]^2 dt'. \quad (7.5)$$

We see that in the presence of a harmonic vector-potential  $\mathbf{A}(t) \propto \sin \omega t$  the phase difference  $\delta\Phi = 0$  vanishes for *all* the loop trajectories with the traversing time equal to the integer period of the time-dependent perturbation:

$$\mathcal{T} = \frac{2\pi n}{\omega}, \quad n = 1, 2, 3... \quad (7.6)$$

Such loop trajectories with the traversing time *synchronized* with the period of perturbation play a crucial role in all the quantum coherence (interference) phenomena in disordered and chaotic systems (their effect on the universal conductance fluctuations has been studied in Ref. [15]). Any periodic in time pertur-

bation leads to a *selection of trajectories*: for strong enough perturbation all trajectories that do not obey Eq.(7.6) do not interfere because of the random phase difference  $\delta\Phi \gg 1$ .

In the particular case of the quantum corrections to the energy absorption rate Eq.(6.2) the time-dependent Cooperon

$$\tilde{C}_{t-t_1/2}(t_1, -t_1) = \exp[-2t_1\Gamma_{t-t_1/2}] \quad (7.7)$$

is small everywhere except for the vicinity of no-dephasing points

$$\omega t_1^{(n)} = 2\omega t - 2\pi n, \quad n = 0, \pm 1, \pm 2 \dots \quad (7.8)$$

For  $\Gamma t_1 \sim \Gamma t \gg 1$  one can expand  $\Gamma_{t-t_1/2} \approx (\omega/2)^2 \Gamma (t_1 - t_1^{(n)})^2$  in the vicinity of no-dephasing points, do the Gaussian integration over  $\zeta = (t_1 - t_1^{(n)})$  and put  $t_1 = t_1^{(n)}$  elsewhere. In particular  $\partial_t \varphi(t - t_1^{(n)}) = -\partial_t \varphi(t)$ . Then we arrive at:

$$\frac{\delta W(t)}{W_0} = -\frac{\delta}{\pi} (2 \sin^2 \omega t) \sum_n \int_{-\infty}^{+\infty} d\zeta e^{-D_E \zeta^2 t_1^{(n)}}. \quad (7.9)$$

Replacing  $\sum_n$  by the integral  $(\omega/2\pi) \int_0^t dt_1$  and averaging over time intervals much larger than  $2\pi/\omega$  we finally get:

$$\frac{W(t)}{W_0} = 1 - \frac{\delta\omega}{\pi} \int_0^t dt_1 \int_{-\infty}^{+\infty} \frac{d\zeta}{2\pi} e^{-D_E \zeta^2 t_1} = 1 - \sqrt{\frac{t}{t_*}}, \quad (7.10)$$

where

$$t_* = \frac{\pi^3 \Gamma}{2\delta^2}. \quad (7.11)$$

We have obtained a remarkable result that the absolute value of the quantum correction to the absorption rate is growing with time. This is the consequence of the existence of no-dephasing points, as otherwise the exponentially decaying Cooperon would lead to a saturation of the integral over  $t_1$  in Eq.(6.2) at large times  $t$ . The negative sign of the correction implies that the absorption rate, or energy diffusion coefficient decreases with time. This phenomenon can be called "weak dynamic localization" in full analogy with the weak Anderson localization when the diffusion coefficient in space is decreasing with the system size. It has been first discovered [16–18] for a simple quantum system – quantum rotor subject to the periodic  $\delta$ -function perturbation. At  $t \sim t_*$  the quantum correction is of the order of the classical Ohmic absorption, and we can expect the strong *dynamic localization* to occur.



Eq.(7.10) suggests a more precise relationship between the dynamic localization for a quantum system in the ergodic (*zero-dimensional*) limit subject to a harmonic perturbation and the Anderson localization in a *quasi-one dimensional* disordered wire. We observe that

$$\partial_t W(t) \propto \int_{-\infty}^{+\infty} \frac{d\zeta}{2\pi} e^{D_E \zeta^2 t} = \int_{-\infty}^{\infty} \frac{d\omega'}{2\pi} e^{-i\omega' t} \int_{-\infty}^{+\infty} \frac{d\zeta}{2\pi} \frac{1}{D_E \zeta^2 - i\omega'}. \quad (7.12)$$

At the same time, according to Eq.(2.22) the correction the (complex) frequency dependent conductivity of an infinite quasi-one dimensional wire is proportional to:

$$\delta\sigma(\omega) = \int_{-\infty}^{+\infty} \frac{dk}{2\pi} \frac{1}{D_0 k^2 - i\omega}. \quad (7.13)$$

We see that the deviation from the no-dephasing points  $\zeta = t_1 - t_1^{(n)}$  is an analogue of the momentum  $k$ . Then with a suitable choice of a time and frequency scale one obtains:

$$\frac{W(t)}{W_0} = \int_{-\infty}^{+\infty} \frac{d\omega'}{2\pi} \frac{e^{-i\omega' t}}{(-i\omega' + 0)} \left( \frac{\sigma(\omega')}{\sigma_0} \right). \quad (7.14)$$

Note that Eq.(7.14) is non-trivial as it establishes a relationship between an essentially non-equilibrium property of a zero-dimensional system and an equilibrium property of a quasi-one dimensional system.

This relationship can be proven for any diagram with an arbitrary number of the Diffuson-Cooperon loops (for the case of two loops see Ref. [19]) and we conjecture that it is *exact* in the ergodic (or random matrix) regime for  $t\Gamma, t\omega \gg 1$ .

Eq.(7.14) helps to establish a character of decay of the absorption rate  $W(t)$  for  $t \gg t_*$ . To this end we recall the Mott-Berezinskii formula for the frequency-dependent conductivity in the localized regime [20]:

$$\sigma(\omega) \propto \omega^2 \ln^2 \omega. \quad (7.15)$$

Then using Eq.(7.14) one obtains the corresponding absorption rate  $W(t)$  at  $t \gg t_*$ :

$$W(t) \propto \frac{\ln t}{t^2}. \quad (7.16)$$

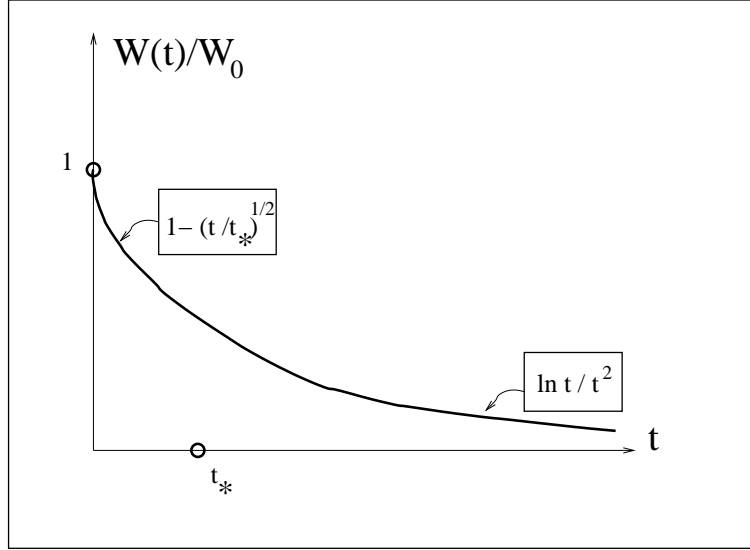


Fig. 21. The time dependence of the absorption rate.

## 8. Conclusion and open questions

The goal of this course was to give a unified picture and a unified theoretical tool to consider different quantum coherence effects in disordered metals. The unified picture is that of interference of electron trajectories with loops traversed in the opposite directions. The corresponding theoretical machinery is the Diffuson-Cooperon diagrammatic technique. We have demonstrated that even the first quantum correction diagram with the Cooperon loop can describe such different and nontrivial phenomena as weak Anderson localization, quantum rectification and dynamic localization in the energy space. We did not try to give a review of the development in the field but rather to concentrate on few important examples and to demonstrate how does the machinery work in different cases. That is why many related issues have not been discussed and the corresponding works have not been cited properly. We apologize for that.

There are few open problems that are related with the main subjects of this school and in our opinion are warrant a study. This is first of all a unified theory of energy absorption where both the Zener transitions picture [21] and the sequential photon absorption picture are incorporated. The suitable theoretical tool for that is believed to be a nonlinear sigma-model in the Keldysh representation derived in Refs. [14]. The perturbative treatment of this field theory

reproduces the diagrammatic technique discussed in this course, and the non-perturbative consideration in the region  $\Gamma, \omega < \delta$  should give the results obtained in the framework of the Zener transitions picture.

Another possible direction is the role of interaction for the quantum rectification and dynamic localization. Some of the interaction effects in dynamic localization have been recently considered in Refs. [22–24] using the Fermi Golden Rule approximation. However, an interesting regime of localization in the Fock space [25] where the Fermi Golden Rule does not apply is awaiting an investigation.

## References

- [1] A. A. Abrikosov, L. P. Gorkov and I. E. Dzyaloshinskii, *Methods of Quantum Field Theory in Statistical Physics*, Pergamon Press, New York (1965).
- [2] L. P. Gor'kov, A. I. Larkin, and D. E. Khmel'nitskii, Pis'ma Zh. Eksp. Teor. Fiz. **30**, 248 (1979) [JETP Lett. **30**, 228 (1979)].
- [3] L. V. Keldysh, Zh. Exp. Teor. Fiz., **47**, 515 (1964) [Sov. Phys.-JETP, **20**, 1018 (1965)].
- [4] J. Rammer and H. Smith, Rev. Mod. Phys., **58**, 323 (1986).
- [5] V. I. Yudson, E. Kanzieper, and V. E. Kravtsov, Phys. Rev. B **64**, 045310 (2001).
- [6] V. E. Kravtsov and V. I. Yudson, Phys. Rev. Lett., **70**, 210 (1993).
- [7] A. G. Aronov and V. E. Kravtsov, Phys. Rev. B, **47**, 13409 (1993).
- [8] V. E. Kravtsov and B. L. Altshuler, Phys. Rev. Lett., **84**, 3394 (2000).
- [9] V. I. Falko and D. E. Khmel'nitskii, Zh. Exp. Teor. Fiz. **95**, 328 (1989) [Sov. Phys.-JETP, **68**, 186 (1989)].
- [10] B. L. Altshuler, A. G. Aronov and D. E. Khmel'nitskii J. Phys. C **15**, 7367 (1982).
- [11] M. G. Vavilov and I. L. Aleiner, Phys. Rev. B **60**, R16311 (1999); **64**, 085115 (2001); M. G. Vavilov, I. L. Aleiner, and V. Ambegaokar, Phys. Rev. B **63**, 195313 (2001).
- [12] M. Büttiker, Y. Imry, and R. Landauer, Phys. Lett. A **96**, 365 (1983).
- [13] L. P. Levy, G. Dolan, J. Dunmuir, and H. Bouchiat, Phys. Rev. Lett., **64**, 2074 (1990).
- [14] D. M. Basko, M. A. Skvortsov and V. E. Kravtsov, Phys. Rev. Lett., **90**, 096801 (2003).
- [15] X.-B. Wang and V. E. Kravtsov, Phys. Rev. B **64**, 033313 (2001); V. E. Kravtsov, Pramana-Journal of Physics, **58**, 183 (2002).
- [16] G. Casati, B. V. Chirikov, J. Ford, and F. M. Izrailev, in *Stochastic Behaviour in Classical and Quantum Hamiltonian Systems*, ed. by G. Casati and J. Ford, Lecture Notes in Physics, vol. 93 (Springer, Berlin, 1979).
- [17] B. V. Chirikov, F. M. Izrailev, and D. L. Shepelyansky, Physica (Amsterdam) **33D**, 77 (1988).
- [18] A. Altland, Phys. Rev. Lett., **71**, 69 (1993).
- [19] M. A. Skvortsov, D. M. Basko and V. E. Kravtsov, JETP Lett., **80**, 60 (2004).
- [20] N. F. Mott, Phys. Mag., **17**, 1259 (1968); V. L. Berezinskii, Zh. Eksp. Teor. Fiz. **65**, 1251 (1973) [Sov. Phys. JETP **38**, 620 (1974)].
- [21] Y. Gefen and D. J. Thouless, Phys. Rev. Lett. **59**, 1752 (1987).
- [22] D. M. Basko, Phys. Rev. Lett., **91**, 206801 (2003).
- [23] D. M. Basko and V. E. Kravtsov, Phys. Rev. Lett., 2004 **93**, 056804.

[24] V.E.Kravtsov, cond-mat/0312316.

[25] B. L. Altshuler, Y. Gefen, A. Kamenev, L. S. Levitov, Phys. Rev. Lett. **78**, 2803 (1997).

This figure "kravtsov.jpg" is available in "jpg" format from:

<http://arxiv.org/ps/cond-mat/0504671v1>